

Journal of Mechanics

<http://journals.cambridge.org/JOM>

Additional services for *Journal of Mechanics*:

Email alerts: [Click here](#)

Subscriptions: [Click here](#)

Commercial reprints: [Click here](#)

Terms of use : [Click here](#)



On Free Vibration of Functionally Graded Mindlin Plate and Effect of In-Plane Displacements

A. Hasani Baferani, A.R. Saidi and H. Ehteshami

Journal of Mechanics / Volume 29 / Issue 02 / June 2013, pp 373 - 384
DOI: 10.1017/jmech.2013.11, Published online: 29 January 2013

Link to this article: http://journals.cambridge.org/abstract_S1727719113000117

How to cite this article:

A. Hasani Baferani, A.R. Saidi and H. Ehteshami (2013). On Free Vibration of Functionally Graded Mindlin Plate and Effect of In-Plane Displacements. Journal of Mechanics, 29, pp 373-384 doi:10.1017/jmech.2013.11

Request Permissions : [Click here](#)

ON FREE VIBRATION OF FUNCTIONALLY GRADED MINDLIN PLATE AND EFFECT OF IN-PLANE DISPLACEMENTS

A. Hasani Baferani

Department of Mechanical Engineering
Amirkabir University of Technology
Hafez Ave., 424, Tehran, Iran

A.R. Saidi* H. Ehteshami

Department of Mechanical Engineering
Shahid Bahonar University of Kerman
Kerman, Iran

ABSTRACT

In this paper, free vibration analysis of functionally graded rectangular plate is investigated based on the first order shear deformation theory and the effect of in-plane displacements on the natural frequencies of such plate is studied. The governing equations of motion are obtained, which are five coupled partial differential equations, without any simplification. Some mathematical manipulation leads us to decouple the equations. The decoupled equations are solved by the Levy's method for various boundary conditions. As the results show, in some boundary conditions the in-plane displacements cause a drastic change of frequencies. In other words, neglecting the in-plane displacement, which is assumed in some papers, is not proper for these boundary conditions. However, in the other boundary conditions, the natural frequencies are not significantly affected by the in-plane displacements. The results for various boundary conditions are discussed in detail and some interpretations for these differences are provided. Besides to the comparisons, the accurate natural frequencies of the plate for six different boundary conditions with several aspect ratios, thickness-length ratios and power law indices are presented. The natural frequencies of Mindlin functionally graded rectangular plates with considering the in-plane displacements are reported for the first time and can be used as benchmark.

Keywords: Free vibration, Functionally graded, In-Plane displacements, Analytical solution.

1. INTRODUCTION

Plates as practical structures have a lot of applications in the various industries such as aerospace, oil installation, *etc.* Surely, the knowledge of dynamic behavior of plates is an essential tool for a designer. The functionally graded materials (FGM's) are newly discovered materials which are used, because of its remarkable mechanical properties, in many engineering applications namely space structures, aerospace and other industries. The mechanical properties of FGM's vary smoothly and continuously from one surface to the other [1-4]. These materials are made from a mixture of metal and ceramic, or a combination of different metals.

Many studies for free vibration analysis of functionally graded (FG) rectangular plates are available in the literature. Yang and Shen [5], based on the classical plate theory, studied the dynamic response of initially stressed functionally graded rectangular thin plates subjected to partially distributed impulsive lateral load. They concluded that the plate with intermediate material properties will have intermediate natural frequencies. He *et al.* [6] investigated the active con-

trol of FG plates with integrated piezoelectric sensors and actuators using the finite element method. Qian *et al.* [7] studied the static and dynamic response of thick FG elastic plates using higher order shear and normal deformation theory. Vel and Batra [8] presented the exact three-dimensional elasticity solution for the vibration of simply supported FG rectangular plates by means of the power series method. Kim [9] studied the temperature dependent vibration of FG rectangular plates. He used the Rayleigh-Ritz method to solve the third order shear deformation plate theory and obtained the dynamic properties. Using finite strip method, Shiau and Zeng [10] studied the free vibration of rectangular plate with delamination. Ferreira *et al.* [11] employed a meshless method to solve the first and the third order shear deformation plate equations and obtained the natural frequencies of FG plates. Based on the first order shear deformation plate theory, Sundarajan *et al.* [12] investigated the nonlinear free flexural vibration of FG rectangular and skew plates in thermal environments. Woo *et al.* [13] presented an analytical solution for the response of nonlinear natural vibration of FG plates. They used the von Karman theory and obtained the solution with

* Corresponding author (saidi@mail.uk.ac.ir)

a semi-analytical method assuming a mixed series solution. They concluded that the fundamental frequency increases with the amplitude of vibration of FG plates due to nonlinear coupling between bending and in-plane stretching. Gilhooley *et al.* [14] studied the free vibration of thick FG plates using higher order shear and normal deformation theory and MLPG method with radial basis functions. Matsunaga [15] obtained the natural frequencies of simply supported FG rectangular plates by means of a two dimensional higher order theory. He concludes that 2-D higher order deformation theory could correctly predict the natural frequency and distribution of displacement and stress components in FG plates. Zhang and Zhou [16] analyzed the vibration of FG thin plates based on the concept of physical neutral surface. They defined a new physical neutral surface and based on this surface, obtained the nonlinear equations of plate. Fares *et al.* [17], using the refined theory, analyzed the free vibration of FG rectangular plates. Malekzadeh [18] studied the free vibration analysis of thick FG simply supported rectangular plates embedded on elastic foundation using the differential quadratic method based on three dimensional elasticity theory. Wu and Lu [19] studied the dynamic response of simply supported-multilayered and magneto-electro elastic FG plates based on the three dimensional elasticity theory. Li *et al.* [20] investigated the three dimensional vibration of FG plates with simply supported and clamped edges in thermal environment. Liu *et al.* [21] assumed the variation of material properties in the plate plane x - y directions and using the classical plate theory and studied the free vibration of FG rectangular plates. Zhao *et al.* [22] performed the free vibration analysis of FG plates using the element free- kp - Ritz method. They used the first order shear deformation plate theory. They concluded that a volume fraction exponent that ranges between 0 and 5 has a significant influence on the frequency, but the effect of the length to thickness ratio on the frequency of a plate are independent of the volume fraction. Hosseini Hashemi *et al.* [23] studied the free vibration of FG rectangular plates for various boundary conditions using first order shear deformation theory. They neglected the in-plane displacement components for finding the governing equations and obtained the natural frequencies of the plate with this simplification. Also, in their last works, Hosseini Hashemi *et al.* [24,25] studied the free vibration of FG rectangular plate based on first and third order shear deformation plate theory. They considered the in-plane displacement components in the governing equations but they present neither results nor discussion on the effects of in-plane displacements.

In present work, free vibration of functionally graded rectangular plates based on the first order shear deformation plate theory is studied. Considering the in-plane displacements, leads to five-coupled partial differential equations. As it also has been stated by some authors, this coupling is emerged due to non-coincidence of mid-plane of plate and physical neutral surface. Consequently, the coupling between bending and stretching appear in the equations of motion.

With some mathematical manipulations, five coupled partial differential equations are converted to decoupled partial differential equations. These equations are solved analytically and the effects of boundary conditions, thickness-length ratio and power law index on natural frequencies of FG rectangular plates are discussed in detail. The novelty of this work is the study of in-plane displacement on natural frequencies of FG rectangular plate with Levy boundary conditions. It has been shown that, for some boundary conditions, the in-plane displacements have significant effects on natural frequencies of functionally graded rectangular plates.

2. THE FORMULATION OF EQUATIONS

A functionally graded rectangular plate of length a , width b and thickness h is considered here. The geometry of the plate and the coordinate system are shown in Fig. 1. The materials at top and bottom surfaces are ceramic and metal, respectively. It is assumed that the overall material properties of the FG plate vary through the thickness coordinate z , ($-h/2 \leq z \leq h/2$) by a power law function as

$$\begin{aligned} E(z) &= E_m + (E_c - E_m) \left(\frac{1}{2} - \frac{z}{h} \right)^n \\ \rho(z) &= \rho_m + (\rho_c - \rho_m) \left(\frac{1}{2} - \frac{z}{h} \right)^n \end{aligned} \quad (1)$$

where $E(z)$ is the Young modulus, $\rho(z)$ is the density and n is the power law index of the plate. The subscripts m and c refer to the metal and ceramic, respectively. Due to the small variations of the Poisson ratio ν , it is assumed to be a constant through the thickness.

Let (u_x, u_y, u_z) be the displacement components of an arbitrary point within the plate domain along the (x, y, z) coordinate directions. According to the first order shear deformation plate theory, the displacement components of the plate in x, y and z directions are assumed to be

$$\begin{aligned} u_x(x, y, z, t) &= u(x, y, t) + z \psi_x(x, y, t) \\ u_y(x, y, z, t) &= v(x, y, t) + z \psi_y(x, y, t) \\ u_z(x, y, z, t) &= w(x, y, t) \end{aligned} \quad (2)$$

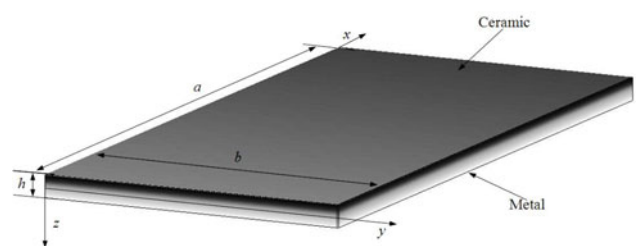


Fig. 1 The geometry and coordinate for FG rectangular plate

where u , v and w are the displacements of the middle surfaces in x , y and z directions and ψ_x and ψ_y are the rotation function of the middle surface. The strain-displacement relations are expressed as

$$\begin{aligned}\varepsilon_{xx} &= \frac{\partial u}{\partial x} + z \frac{\partial \psi_x}{\partial x} \\ \varepsilon_{yy} &= \frac{\partial v}{\partial y} + z \frac{\partial \psi_y}{\partial y} \\ 2\varepsilon_{xy} &= \frac{\partial u}{\partial y} + \frac{\partial v}{\partial x} + z \left(\frac{\partial \psi_x}{\partial y} + \frac{\partial \psi_y}{\partial x} \right) \\ 2\varepsilon_{xz} &= \frac{\partial w}{\partial x} + \psi_x \\ 2\varepsilon_{yz} &= \frac{\partial w}{\partial y} + \psi_y\end{aligned}\quad (3)$$

where ε_{xx} and ε_{yy} are the normal strains and ε_{xy} , ε_{xz} and ε_{yz} are the shear strains components. Considering the Hooke's law, the stress-strain relations are as follows

$$\begin{aligned}\sigma_{xx} &= \frac{E(z)}{1-\nu^2} (\varepsilon_{xx} + \nu \varepsilon_{yy}) \\ \sigma_{yy} &= \frac{E(z)}{1-\nu^2} (\varepsilon_{yy} + \nu \varepsilon_{xx}) \\ \sigma_{xy} &= \frac{E(z)}{2(1+\nu)} (2\varepsilon_{xy}) \\ \sigma_{yz} &= \frac{E(z)}{2(1+\nu)} (2\varepsilon_{yz}) \\ \sigma_{xz} &= \frac{E(z)}{2(1+\nu)} (2\varepsilon_{xz})\end{aligned}\quad (4)$$

where σ_{xx} , σ_{yy} and σ_{xy} , σ_{xz} , σ_{yz} are the normal and shear stress components, respectively. By means of the displacement field (2) and Eqs. (3), and using the Hamilton's principle, the equations of motion are obtained as [26,27]

$$\begin{aligned}\frac{\partial N_{xx}}{\partial x} + \frac{\partial N_{xy}}{\partial y} &= I_0 \ddot{u} + I_1 \ddot{\psi}_x \\ \frac{\partial N_{xy}}{\partial x} + \frac{\partial N_{yy}}{\partial y} &= I_0 \ddot{v} + I_1 \ddot{\psi}_y \\ \frac{\partial M_{xx}}{\partial x} + \frac{\partial M_{xy}}{\partial y} - Q_x &= I_1 \ddot{u} + I_2 \ddot{\psi}_x \\ \frac{\partial M_{xy}}{\partial x} + \frac{\partial M_{yy}}{\partial y} - Q_y &= I_1 \ddot{v} + I_2 \ddot{\psi}_y \\ \frac{\partial Q_x}{\partial x} + \frac{\partial Q_y}{\partial y} &= I_0 \ddot{w}\end{aligned}\quad (5)$$

In the above equations the superscript dot denotes partial differentiating with respect to time ($(\dot{\quad}) = \partial(\quad)/\partial t$). Also, I_i ($i = 0, 1, 2$) are the inertia terms. N_{xx} , N_{yy} and N_{xy} are the in-plane resultant forces, M_{xx} , M_{yy} and M_{xy} are the bending and twisting moment intensities and Q_x and Q_y are the out of plane resultant forces. These parameters are defined as

$$\begin{aligned}(N_{xx}, N_{yy}, N_{xy}) &= \int_{-h/2}^{h/2} (\sigma_{xx}, \sigma_{yy}, \sigma_{xy}) dz \\ (M_{xx}, M_{yy}, M_{xy}) &= \int_{-h/2}^{h/2} (\sigma_{xx}, \sigma_{yy}, \sigma_{xy}) z dz \\ (Q_x, Q_y) &= k^2 \int_{-h/2}^{h/2} (\sigma_{xz}, \sigma_{yz}) dz \\ (I_0, I_1, I_2) &= \int_{-h/2}^{h/2} \rho(z) (1, z, z^2) dz\end{aligned}\quad (6)$$

In the third equation of (6), k^2 is the shear correction factor, which is assumed to be $5/6$. Substituting Eqs. (1), (3) and (4) into Eq. (6) give the following relations for resultant forces and moments

$$\begin{aligned}N_{xx} &= A_{11} \frac{\partial u}{\partial x} + A_{12} \frac{\partial v}{\partial y} + B_{11} \frac{\partial \psi_x}{\partial x} + B_{12} \frac{\partial \psi_y}{\partial y} \\ N_{yy} &= A_{11} \frac{\partial v}{\partial y} + A_{12} \frac{\partial u}{\partial x} + B_{11} \frac{\partial \psi_y}{\partial y} + B_{12} \frac{\partial \psi_x}{\partial x} \\ N_{xy} &= A_{33} \left(\frac{\partial u}{\partial y} + \frac{\partial v}{\partial x} \right) + B_{33} \left(\frac{\partial \psi_x}{\partial y} + \frac{\partial \psi_y}{\partial x} \right) \\ M_{xx} &= B_{11} \frac{\partial u}{\partial x} + B_{12} \frac{\partial v}{\partial y} + D_{11} \frac{\partial \psi_x}{\partial x} + D_{12} \frac{\partial \psi_y}{\partial y} \\ M_{yy} &= B_{11} \frac{\partial v}{\partial y} + B_{12} \frac{\partial u}{\partial x} + D_{11} \frac{\partial \psi_y}{\partial y} + D_{12} \frac{\partial \psi_x}{\partial x} \\ M_{xy} &= B_{33} \left(\frac{\partial u}{\partial y} + \frac{\partial v}{\partial x} \right) + D_{33} \left(\frac{\partial \psi_x}{\partial y} + \frac{\partial \psi_y}{\partial x} \right) \\ Q_x &= k^2 A_{33} \left(\psi_x + \frac{\partial w}{\partial x} \right) \\ Q_y &= k^2 A_{33} \left(\psi_y + \frac{\partial w}{\partial y} \right)\end{aligned}\quad (7)$$

where A_ξ , B_ξ , D_ξ ($\xi = 11, 12, 33$) are the material stiffness coefficients of the plate which can be defined in the form of

$$\begin{aligned}(A_{11}, B_{11}, D_{11}) &= \int_{-h/2}^{h/2} \frac{E(z)}{1-\nu^2} (1, z, z^2) dz \\ (A_{12}, B_{12}, D_{12}) &= \int_{-h/2}^{h/2} \frac{\nu E(z)}{1-\nu^2} (1, z, z^2) dz \\ (A_{33}, B_{33}, D_{33}) &= \int_{-h/2}^{h/2} \frac{E(z)}{2(1+\nu)} (1, z, z^2) dz\end{aligned}\quad (8)$$

Substituting the resultant forces and moments obtained from Eqs. (7) into Eqs. (5), the governing equations of motion for a FG rectangular plate are obtained as

$$\begin{aligned}
& A_{11} \left(\frac{\partial^2 u}{\partial x^2} + \frac{\partial^2 v}{\partial x \partial y} \right) + A_{33} \left(\frac{\partial^2 u}{\partial y^2} - \frac{\partial^2 v}{\partial x \partial y} \right) + B_{11} \left(\frac{\partial^2 \psi_x}{\partial x^2} + \frac{\partial^2 \psi_y}{\partial x \partial y} \right) + B_{33} \left(\frac{\partial^2 \psi_x}{\partial y^2} - \frac{\partial^2 \psi_y}{\partial x \partial y} \right) = I_0 \ddot{u} + I_1 \ddot{\psi}_x \\
& A_{11} \left(\frac{\partial^2 v}{\partial y^2} + \frac{\partial^2 u}{\partial x \partial y} \right) + A_{33} \left(\frac{\partial^2 v}{\partial x^2} - \frac{\partial^2 u}{\partial x \partial y} \right) + B_{11} \left(\frac{\partial^2 \psi_y}{\partial y^2} + \frac{\partial^2 \psi_x}{\partial x \partial y} \right) + B_{33} \left(\frac{\partial^2 \psi_y}{\partial x^2} - \frac{\partial^2 \psi_x}{\partial x \partial y} \right) = I_0 \ddot{v} + I_1 \ddot{\psi}_y \\
& B_{11} \left(\frac{\partial^2 u}{\partial x^2} + \frac{\partial^2 v}{\partial x \partial y} \right) + B_{33} \left(\frac{\partial^2 u}{\partial y^2} - \frac{\partial^2 v}{\partial x \partial y} \right) + D_{11} \left(\frac{\partial^2 \psi_x}{\partial x^2} + \frac{\partial^2 \psi_y}{\partial x \partial y} \right) + D_{33} \left(\frac{\partial^2 \psi_x}{\partial y^2} - \frac{\partial^2 \psi_y}{\partial x \partial y} \right) \\
& - k^2 A_{33} \left(\psi_x + \frac{\partial w}{\partial x} \right) = I_1 \ddot{u} + I_2 \ddot{\psi}_x \\
& B_{11} \left(\frac{\partial^2 v}{\partial y^2} + \frac{\partial^2 u}{\partial x \partial y} \right) + B_{33} \left(\frac{\partial^2 v}{\partial x^2} - \frac{\partial^2 u}{\partial x \partial y} \right) + D_{11} \left(\frac{\partial^2 \psi_y}{\partial y^2} + \frac{\partial^2 \psi_x}{\partial x \partial y} \right) + D_{33} \left(\frac{\partial^2 \psi_y}{\partial x^2} - \frac{\partial^2 \psi_x}{\partial x \partial y} \right) \\
& - k^2 A_{33} \left(\psi_y + \frac{\partial w}{\partial y} \right) = I_1 \ddot{v} + I_2 \ddot{\psi}_y \\
& k^2 A_{33} \left(\frac{\partial^2 w}{\partial x^2} + \frac{\partial^2 w}{\partial y^2} + \frac{\partial \psi_x}{\partial x} + \frac{\partial \psi_y}{\partial y} \right) = I_0 \ddot{w}
\end{aligned} \tag{9}$$

Equations (9) are five highly coupled partial differential equations in terms of in-plane displacements, rotation functions and transverse displacements. These equations can not be solved easily. For solving these equations analytically, it is desirable to find a method for decoupling them. Using the following analytical method, these governing equations will be decoupled. Equations (9) can be easily rewritten in the form

$$\begin{aligned}
& A_{11} \frac{\partial \phi_1}{\partial x} + A_{33} \frac{\partial \phi_2}{\partial y} + B_{11} \frac{\partial \phi_3}{\partial x} + B_{33} \frac{\partial \phi_4}{\partial y} = I_0 \ddot{u} + I_1 \ddot{\psi}_x \\
& A_{11} \frac{\partial \phi_1}{\partial y} - A_{33} \frac{\partial \phi_2}{\partial x} + B_{11} \frac{\partial \phi_3}{\partial y} - B_{33} \frac{\partial \phi_4}{\partial x} = I_0 \ddot{v} + I_1 \ddot{\psi}_y \\
& B_{11} \frac{\partial \phi_1}{\partial x} + B_{33} \frac{\partial \phi_2}{\partial y} + D_{11} \frac{\partial \phi_3}{\partial x} + D_{33} \frac{\partial \phi_4}{\partial y} - k^2 A_{33} \left(\psi_x + \frac{\partial w}{\partial x} \right) = I_1 \ddot{u} + I_2 \ddot{\psi}_x \\
& B_{11} \frac{\partial \phi_1}{\partial y} - B_{33} \frac{\partial \phi_2}{\partial x} + D_{11} \frac{\partial \phi_3}{\partial y} - D_{33} \frac{\partial \phi_4}{\partial x} - k^2 A_{33} \left(\psi_y + \frac{\partial w}{\partial y} \right) = I_1 \ddot{v} + I_2 \ddot{\psi}_y \\
& k^2 A_{33} (\nabla^2 w + \phi_3) = I_0 \ddot{w}
\end{aligned} \tag{10}$$

where ∇^2 is the two dimensional Laplace operator and the variables ϕ_1 , ϕ_2 , ϕ_3 and ϕ_4 are defined as

$$\begin{aligned}
\phi_1 &= \frac{\partial u}{\partial x} + \frac{\partial v}{\partial y} \\
\phi_2 &= \frac{\partial u}{\partial y} - \frac{\partial v}{\partial x} \\
\phi_3 &= \frac{\partial \psi_x}{\partial x} + \frac{\partial \psi_y}{\partial y} \\
\phi_4 &= \frac{\partial \psi_x}{\partial y} - \frac{\partial \psi_y}{\partial x}
\end{aligned} \tag{11}$$

Also Eqs. (10a) and (10b) are rewritten in the form

$$\begin{aligned}
& B_{11} \frac{\partial \phi_1}{\partial x} + B_{33} \frac{\partial \phi_2}{\partial y} = -\frac{B_{11}^2}{A_{11}} \frac{\partial \phi_3}{\partial x} - \frac{B_{11} B_{33}}{A_{11}} \frac{\partial \phi_4}{\partial y} + \frac{B_{11}}{A_{11}} (I_0 \ddot{u} + I_1 \ddot{\psi}_x) \\
& B_{11} \frac{\partial \phi_1}{\partial y} - B_{33} \frac{\partial \phi_2}{\partial x} = -\frac{B_{11}^2}{A_{11}} \frac{\partial \phi_3}{\partial y} + \frac{B_{11} B_{33}}{A_{11}} \frac{\partial \phi_4}{\partial x} + \frac{B_{11}}{A_{11}} (I_0 \ddot{v} + I_1 \ddot{\psi}_y)
\end{aligned} \tag{12}$$

Substituting Eqs. (12) into Eqs. (10c) and (10d) give us the following relations

$$\begin{aligned} \left(D_{11} - \frac{B_{11}^2}{A_{11}} \right) \frac{\partial \varphi_3}{\partial x} + \left(D_{33} - \frac{B_{11} B_{33}}{A_{11}} \right) \frac{\partial \varphi_4}{\partial y} \\ - k^2 A_{33} \left(\frac{\partial w}{\partial x} + \psi_x \right) = J_1 \ddot{u} + J_2 \ddot{\psi}_x \\ \left(D_{11} - \frac{B_{11}^2}{A_{11}} \right) \frac{\partial \varphi_3}{\partial y} - \left(D_{33} - \frac{B_{11} B_{33}}{A_{11}} \right) \frac{\partial \varphi_4}{\partial x} \\ - k^2 A_{33} \left(\frac{\partial w}{\partial y} + \psi_y \right) = J_1 \ddot{v} + J_2 \ddot{\psi}_y \end{aligned} \quad (13)$$

where the parameters J_1 and J_2 are defined as

$$\begin{aligned} J_1 &= I_1 - \frac{B_{11}}{A_{11}} I_0 \\ J_2 &= I_2 - \frac{B_{11}}{A_{11}} I_1 \end{aligned} \quad (14)$$

By differentiating the Eqs. (13a) and (13b) with respect to x and y and doing some algebraic operations, the following partial differential equations are obtained

$$\begin{aligned} \hat{D} \nabla^2 \varphi_3 - k^2 A_{33} (\nabla^2 w + \varphi_3) = J_1 \ddot{\phi}_1 + J_2 \ddot{\phi}_3 \\ \hat{C} \nabla^2 \varphi_4 - k^2 A_{33} \varphi_4 = J_1 \ddot{\phi}_2 + J_2 \ddot{\phi}_4 \end{aligned} \quad (15)$$

where the parameters \hat{D} and \hat{C} are defined as

$$\begin{aligned} \hat{D} &= D_{11} - \frac{B_{11}^2}{A_{11}} \\ \hat{C} &= D_{33} - \frac{B_{11} B_{33}}{A_{11}} \end{aligned} \quad (16)$$

Similarly, differentiating Eqs. (10a) and (10b) with respect to x and y and doing some algebraic calculations, these equations are obtained

$$\begin{aligned} A_{11} \nabla^2 \varphi_1 + B_{11} \nabla^2 \varphi_3 = I_1 \ddot{\phi}_1 + I_2 \ddot{\phi}_3 \\ A_{33} \nabla^2 \varphi_2 + B_{33} \nabla^2 \varphi_4 = I_1 \ddot{\phi}_2 + I_2 \ddot{\phi}_4 \end{aligned} \quad (17)$$

By considering the equations of motion (5) and doing some algebraic operations, the following partial differential equations are obtained in the form

$$\begin{aligned} \lambda_1 \nabla^6 w + \lambda_2 \nabla^4 \dot{w} + \lambda_3 \nabla^2 \ddot{w} + \lambda_4 \nabla^2 \dot{\psi} + \lambda_5 \ddot{\psi} + \lambda_6 \ddot{\psi} = 0 \\ \lambda_7 \nabla^4 \varphi_4 + \lambda_8 \nabla^2 \varphi_4 + \lambda_9 \nabla^2 \dot{\varphi}_4 + \lambda_{10} \ddot{\varphi}_4 + \lambda_{11} \ddot{\varphi}_4 = 0 \end{aligned} \quad (18)$$

where the parameters λ_i ($i = 1$ to 11) are defined as

$$\begin{aligned} \lambda_1 &= \frac{\hat{D} A_{11}}{J_1} \quad \lambda_2 = \frac{\hat{D} I_0}{J_1} + \frac{\hat{D} I_0 A_{11}}{J_1 k^2 A_{33}} + \frac{J_2 A_{11}}{J_1} - B_{11} \\ \lambda_3 &= -\frac{I_0 A_{11}}{J_1} \quad \lambda_4 = \frac{I_0 J_2 A_{11}}{k^2 A_{33} J_1} - \frac{I_0 B_{11}}{k^2 A_{33}} + \frac{I_0^2 \hat{D}}{k^2 A_{33} J_1} + \frac{I_0 J_2}{J_1} - I_1 \\ \lambda_5 &= -\frac{I_0^2}{J_1} \quad \lambda_6 = \frac{I_0^2 J_2}{J_1 k^2 A_{33}} - \frac{I_0 I_1}{k^2 A_{33}} \end{aligned}$$

$$\begin{aligned} \lambda_7 &= -\frac{\hat{C} A_{33}}{J_1} \quad \lambda_8 = \frac{k^2 A_{33}^2}{J_1} \\ \lambda_9 &= B_{33} - \frac{J_2 A_{33}}{J_1} - \frac{I_0 \hat{C}}{J_1} \quad \lambda_{10} = \frac{k^2 A_{33} I_0}{J_1} \\ \lambda_{11} &= I_1 - \frac{I_0 J_2}{J_1} \end{aligned} \quad (19)$$

Equation (18) are two uncoupled partial differential equations in terms of transverse displacement w and a new function φ_4 . Using these equations, the free vibration analysis of FG rectangular plates could be analytically investigated.

3. LEVY SOLUTION

To solve Eq. (18), let us consider a FG rectangular plate with simply supported boundary conditions at two x -direction edges and arbitrary boundary conditions at the other edges. Then, the transverse displacement w and function φ_4 can be assumed to be

$$\begin{aligned} w &= \sum_{m=1}^{\infty} w_m(y) \sin(\mu_m x) e^{i\omega_m t} \\ \varphi_4 &= \sum_{m=1}^{\infty} \varphi_m(y) \cos(\mu_m x) e^{i\omega_m t} \end{aligned} \quad (20)$$

where ω_m is the natural frequency and μ_m denotes $m\pi/a$. Substituting the proposed series solutions (20) into the decoupled Eq. (18), yields

$$\begin{aligned} \gamma_1 \frac{d^6 w_m}{dy^6} + \gamma_2 \frac{d^4 w_m}{dy^4} + \gamma_3 \frac{d^2 w_m}{dy^2} + \gamma_4 w_m(y) = 0 \\ \gamma_5 \frac{d^4 \varphi_m}{dy^4} + \gamma_6 \frac{d^2 \varphi_m}{dy^2} + \gamma_7 \varphi_m(y) = 0 \end{aligned} \quad (21)$$

where the parameters γ_i ($i = 1 \dots 7$) are defined as

$$\begin{aligned} \gamma_1 &= \frac{A_{11} \hat{D}}{J_1 \omega_m^2} \\ \gamma_2 &= \frac{A_{11} \hat{D} I_0}{J_1 k^2 A_{33}} + \frac{I_0 \hat{D}}{J_1} + \frac{A_{11} I_2}{J_1} - B_{11} - \frac{3 A_{11} \hat{D} \mu_m^2}{J_1 \omega_m^2} - \frac{B_{11} I_1}{J_1} \\ \gamma_3 &= \frac{\omega_m^2 I_0 I_2}{J_1} - \frac{A_{11} I_0}{J_1} - \frac{B_{11} I_0 \omega_m^2}{k^2 A_{33}} + \frac{A_{11} \omega_m^2 I_2 I_0}{J_1 k^2 A_{33}} \\ &+ \frac{\omega_m^2 I_0^2 \hat{D}}{J_1 k^2 A_{33}} - \frac{\omega_m^2 B_{11} I_1 I_0}{J_1 k^2 A_{33}} - \frac{2 I_0 \hat{D} \mu_m^2}{J_1} \\ &+ \frac{2 B_{11} I_1 \mu_m^2}{J_1} - \frac{2 A_{11} \hat{D} I_0 \mu_m^2}{J_1 k^2 A_{33}} - \frac{2 A_{11} I_2 \mu_m^2}{J_1} - I_1 \omega_m^2 \\ &+ 2 B_{11} \mu_m^2 + \frac{3 A_{11} \hat{D} \mu_m^4}{J_1 \omega_m^2} - \frac{\omega_m^2 I_0 B_{11} I_1}{J_1 A_{11}} \end{aligned}$$

$$\begin{aligned} \gamma_4 = & \omega_m^2 I_1 \mu_m^2 - \frac{\omega_m^4 I_1 I_0}{k^2 A_{33}} + \frac{\omega_m^4 I_0^2 I_2}{J_1 k^2 A_{33}} - \frac{\omega_m^2 I_0^2}{J_1} \\ & - \frac{\omega_m^4 I_0^2 B_{11} I_1}{J_1 k^2 A_{33} A_{11}} - \frac{\omega_m^2 I_0^2 \hat{D} \mu_m^2}{J_1 k^2 A_{33}} - \frac{\omega_m^2 I_0 I_2 \mu_m^2}{J_1} \\ & - \mu_m^4 B_{11} - \frac{\mu_m^4 B_{11} I_1}{J_1} + \frac{A_{11} I_0 \mu_m^2}{J_1} + \frac{\mu_m^2 I_0 B_{11} I_1 \omega_m^2}{J_1 A_{11}} \\ & + \frac{B_{11} \omega_m^2 I_1 I_0 \mu_m^2}{J_1 k^2 A_{33}} + \frac{B_{11} I_0 \omega_m^2 \mu_m^2}{k^2 A_{33}} + \frac{A_{11} \hat{D} I_0 \mu_m^4}{J_1 k^2 A_{33}} \\ & + \frac{\mu_m^4 \hat{D} I_0}{J_1} - \frac{A_{11} \hat{D} \mu_m^6}{J_1 \omega_m^2} - \frac{A_{11} \omega_m^2 I_0 I_2 \mu_m^2}{J_1 k^2 A_{33}} + \frac{A_{11} I_2 \mu_m^4}{J_1} \end{aligned} \quad (22)$$

$$\gamma_5 = -A_{11} A_{33} \hat{C}$$

$$\begin{aligned} \gamma_6 = & A_{33} B_{11} I_1 \omega_m^2 + k^2 A_{33}^2 A_{11} - A_{33} I_2 \omega_m^2 A_{11} \\ & + B_{33} \omega_m^2 J_1 A_{11} + 2 A_{33} \hat{C} \mu_m^2 A_{11} - I_0 \hat{C} \omega_m^2 A_{11} \end{aligned}$$

$$\begin{aligned} \gamma_7 = & I_0 B_{11} I_1 \omega_m^4 + I_0 k^2 A_{33} A_{11} \omega_m^2 - A_{33} \hat{C} A_{11} \mu_m^4 \\ & - A_{33} B_{11} I_1 \mu_m^2 \omega_m^2 - k^2 A_{33}^2 A_{11} \mu_m^2 + A_{33} I_2 A_{11} \omega_m^2 \mu_m^2 \\ & - B_{33} J_1 A_{11} \mu_m^2 \omega_m^2 + I_1 J_1 A_{11} \omega_m^4 \\ & + I_0 A_{11} \hat{C} \mu_m^2 \omega_m^2 - I_0 I_2 A_{11} \omega_m^4 \end{aligned}$$

Equation (21) are two ordinary differential equations in terms of w_m and φ_m . The solutions of these differential equations are as follows

$$\begin{aligned} w_m(y) = & C_1 \sinh(\chi_1 y) + C_2 \cosh(\chi_1 y) + C_3 \sinh(\chi_2 y) \\ & + C_4 \cosh(\chi_2 y) + C_5 \sinh(\chi_3 y) + C_6 \cosh(\chi_3 y) \\ \varphi_m(y) = & C_7 \sinh(\chi_4 y) + C_8 \cosh(\chi_4 y) \\ & + C_9 \sinh(\chi_5 y) + C_{10} \cosh(\chi_5 y) \end{aligned} \quad (23)$$

where the parameters χ_i ($i = 1 \dots 5$) are defined as

$$\chi_1 = \frac{1}{6\gamma_1 T} \sqrt{-3\gamma_1 T(-12T\gamma_1 \mu_m^2 + T^2 - 12\gamma_1 \gamma_3 + 4\gamma_2^2 - 4i\sqrt{3}\gamma_2^2 + 4T\gamma_2 + \sqrt{3}T^2 i + 12i\sqrt{3}\gamma_1 \gamma_3)} \quad (24a)$$

$$\chi_2 = \frac{1}{6\gamma_1 T} \sqrt{3\gamma_1 T(12T\gamma_1 \mu_m^2 - T^2 + 12\gamma_1 \gamma_3 - 4\gamma_2^2 - 4i\sqrt{3}\gamma_2^2 - 4T\gamma_2 + \sqrt{3}T^2 i + 12i\sqrt{3}\gamma_1 \gamma_3)} \quad (24b)$$

$$\chi_3 = \frac{1}{6\gamma_1 T} \sqrt{-6\gamma_1 T(-6T\gamma_1 \mu_m^2 - T^2 + 12\gamma_1 \gamma_3 - 4\gamma_2^2 + 2T\gamma_2)} \quad (24c)$$

$$\chi_4 = \frac{1}{2\gamma_5} \sqrt{2\gamma_5(2\gamma_5 \mu_m^2 - \gamma_6 + \sqrt{\gamma_6^2 - 4\gamma_5 \gamma_7})} \quad (24d)$$

$$\chi_5 = \frac{1}{2\gamma_5} \sqrt{-2\gamma_5(-2\gamma_5 \mu_m^2 + \gamma_6 + \sqrt{\gamma_6^2 - 4\gamma_5 \gamma_7})} \quad (24e)$$

In the above equations, $i = \sqrt{-1}$ and the parameter T is defined as

$$T = (36\gamma_1 \gamma_3 \gamma_2 - 108\gamma_4 \gamma_1^2 - 8\gamma_2^3 + 12\sqrt{3}\gamma_1 \sqrt{4\gamma_1 \gamma_3^3 - \gamma_3^2 \gamma_2^2 - 18\gamma_1 \gamma_3 \gamma_2 \gamma_4 + 27\gamma_3^2 \gamma_1^2 + 4\gamma_3 \gamma_2^3})^{\frac{1}{3}} \quad (25)$$

The solution (23) are valid for real parameters χ_i ($i = 1 \dots 4$). When these parameters become imaginary, their corresponding terms *sinh* and *cosh* in Eqs. (23) are converted into *sin* and *cos*.

By using the equations of motion (10) and doing some algebraic calculations, the in plane displacements and rotation functions are obtained as

$$u = \frac{1}{O_5} \left(O_1 \frac{\partial \varphi_1}{\partial x} + O_2 \frac{\partial \varphi_2}{\partial y} + O_3 \frac{\partial \varphi_3}{\partial x} + O_4 \frac{\partial \varphi_4}{\partial y} - (k^2 A_{33} I_1 \omega_m^2) \frac{\partial w}{\partial x} \right) \quad (26a)$$

$$v = \frac{1}{O_5} \left(O_1 \frac{\partial \varphi_1}{\partial y} - O_2 \frac{\partial \varphi_2}{\partial x} + O_3 \frac{\partial \varphi_3}{\partial y} - O_4 \frac{\partial \varphi_4}{\partial x} - (k^2 A_{33} I_1 \omega_m^2) \frac{\partial w}{\partial y} \right) \quad (26b)$$

$$\begin{aligned} \psi_x = & \frac{1}{O_6} \left((A_{11} I_1 - B_{11} I_0) \frac{\partial \varphi_1}{\partial x} + (A_{33} I_1 - B_{33} I_0) \frac{\partial \varphi_2}{\partial y} + (B_{11} I_1 - D_{11} I_0) \frac{\partial \varphi_3}{\partial x} \right. \\ & \left. + (B_{33} I_1 - D_{33} I_0) \frac{\partial \varphi_4}{\partial y} + (k^2 A_{33} I_0) \frac{\partial w}{\partial x} \right) \end{aligned} \quad (26c)$$

$$\Psi_y = \frac{1}{O_6} \left((A_{11} I_1 - B_{11} I_0) \frac{\partial \phi_1}{\partial y} - (A_{33} I_1 - B_{33} I_0) \frac{\partial \phi_2}{\partial x} + (B_{11} I_1 - D_{11} I_0) \frac{\partial \phi_3}{\partial y} - (B_{33} I_1 - D_{33} I_0) \frac{\partial \phi_4}{\partial x} + (k^2 A_{33} I_0) \frac{\partial w}{\partial y} \right) \quad (26d)$$

where the parameters O_i ($i = 1 \dots 6$) are defined as

$$\begin{aligned} O_1 &= (k^2 A_{33} - I_2 \omega_m^2) A_{11} + B_{11} I_1 \omega_m^2 \\ O_2 &= (k^2 A_{33} - I_2 \omega_m^2) A_{33} + B_{33} I_1 \omega_m^2 \\ O_3 &= (k^2 A_{33} - I_2 \omega_m^2) B_{11} + D_{11} I_1 \omega_m^2 \\ O_4 &= (k^2 A_{33} - I_2 \omega_m^2) B_{33} + D_{33} I_1 \omega_m^2 \\ O_5 &= -(I_1^2 \omega_m^4 + I_0 \omega_m^2 (k^2 A_{33} - I_2 \omega_m^2)) \\ O_6 &= O_5 / \omega_m^2 \end{aligned} \quad (27)$$

4. BOUNDARY CONDITIONS

Here, six possible boundary conditions are considered, which are combinations of simply supported, clamped and free at the y -direction edges.

For simply supported edges, the boundary conditions can be rewritten as

$$w = M_{yy} = \psi_x = N_{yy} = u = 0 \quad (28)$$

For clamped boundary conditions, it can be concluded that

$$w = \psi_x = \psi_y = u = v = 0 \quad (29)$$

and the boundary conditions for free edges are

$$M_{yy} = M_{xy} = N_{yy} = N_{xy} = Q_y = 0 \quad (30)$$

where

$$Q_y = k^2 A_{33} \left(\psi_y + \frac{\partial w}{\partial y} \right) \quad (31)$$

Applying arbitrary boundary conditions at two edges of the FG plate in y -direction, a system of ten homogeneous algebraic equations is obtained. Setting the determinant of coefficient matrix equal to zero, the natural frequencies of the plate can be determined.

5. NUMERICAL RESULTS AND DISCUSSION

For numerical calculations, a functionally graded plate composed of aluminum (as metal) and alumina (as ceramic) is considered. The material properties have been listed in Table 1. The Poisson's ratio of the plate is assumed to be constant through the thickness and equal to 0.3. In order to validate the accuracy of the present work, the numerical results for simply supported FG rectangular plates are compared with the available results in Refs. [15] and [22]. It can be seen from Table 2 that the present results are in a good agreement with the results of Matsunaga [15] and Zhao *et al.* [22].

Table 1 Properties of the FGM components

Material	Properties		
	$E(\text{N/m}^2)$	ν	$\rho(\text{Kg/m}^3)$
Aluminum (Al)	70×10^9	0.3	2707
Alumina (Al_2O_3)	380×10^9	0.3	3800
Zirconia (ZrO_2)	200×10^9	0.3	5700

Table 2 Comparison of the non-dimensional fundamental frequency $\varpi = \omega h \sqrt{\rho_c / E_c}$ for simply supported Al / Al_2O_3 square FG plate

h/a		$n = 0$	$n = 0.5$	$n = 1$	$n = 4$	$n = 10$
0.1	Zhao <i>et al.</i> (2009)	0.05673	0.04818	0.04346	0.03757	0.03591
	Matsunaga (2008)	0.05777	0.04917	0.04426	0.03811	0.03642
	Present	0.05768	0.04898	0.04417	0.03820	0.03655
0.2	Zhao <i>et al.</i> (2009)	0.2055	0.1757	0.1587	0.1356	0.1284
	Matsunaga (2008)	0.2121	0.1819	0.1640	0.1383	0.1306
	Present	0.21116	0.18044	0.1630	0.13956	0.13226

The boundary conditions are identified according to the edges of the plate (*e.g.* SCSF denotes simply supported boundary conditions in x -direction and clamped and free boundary conditions in y -direction). Here, six possible boundary conditions for FG rectangular plate containing SCSC, SCSS, SCSF, SSSF, SSSS and SFSF have been considered.

To study the effects of in-plane displacements on the natural frequencies of FG rectangular plates, Tables 3 through 8 have been presented. In these tables, the non-dimensional frequency $\varpi = \omega h \sqrt{\rho_c / E_c}$ is given for all possible boundary conditions versus h/a and a/b .

The results have also been compared with those reported with ignoring the in-plane displacements by Hosseini-Hashemi *et al.* [23]. It can be seen from Table 3 that for the SSSS boundary condition the difference between our results and those of Ref. [23] is not great. However, in the case of aspect ratio equal to 2, 12.25% difference is seen. From Table 3 it can

Table 3 Effect of in-plane displacements on non-dimensional fundamental frequency $\omega = \omega h \sqrt{\rho_c / E_c}$ of SSSS and SSSC Al / Al_2O_3 FG plate versus a/b and n ($h/a = 0.15$)

a/b	n	Hosseini-Hashemi <i>et al.</i> (2010)	SSSS	Difference (%)	Hosseini-Hashemi <i>et al.</i> (2010)	SSSC	Difference (%)
0.5	0	0.08006	0.08006	0	0.08325	0.08325	0
	0.25	0.07320	0.07323	0.041	0.07600	0.07617	0.223
	1	0.06335	0.06141	-3.16	0.06541	0.063915	-2.34
	5	0.05379	0.05253	-2.398	0.05524	0.054615	-1.144
1	0	0.12480	0.12480	0	0.14378	0.14379	0
	0.25	0.11354	0.11427	0.6388	0.12974	0.13191	1.645
	1	0.09644	0.09595	-0.51	0.10725	0.111105	3.47
	5	0.08027	0.08175	1.844	0.08720	0.094110	7.342
2	0	0.28513	0.28513	0	0.35045	0.35045	0
	0.25	0.25555	0.26199	2.458	0.30709	0.323775	5.153
	1	0.20592	0.220935	6.8	0.23262	0.27555	15.58
	5	0.16315	0.185910	12.242	0.17691	0.228135	18.59

be observed that differences in the SSSC boundary condition, especially for the greater power law index and aspect ratio, is significant. Such phenomena is expectable, because the increase of the power index leads to replacing the neural surface to a place which is far from the mid-plane and the increase of the aspect ratio leads to increase the length of the clamped edge. The maximum differences (absolute value) for aspect ratios 0.5, 1 and 2 occur in the power index 1, 5 and 5, respectively. In the Table 4, the natural frequencies and their comparison with Ref. [23] for SCSC and SSSF boundary conditions have been presented. As it can be seen from this table, for the SCSC boundary conditions, with the increase of power index and aspect ratio the differences increase. The reasons are the same as those presented for the case of SSSC boundary condition. However, it is worthy to mention that differences in this case are higher than SSSC. For the aspect ratios 1 and 2 and the power index 5, the differences are as high as 13.28% and 29.55%, respectively. With the same power index and aspect ratios for the case of SSSC, the differences are 7.34% and 18.59%. These major discrepancies are due to increasing the length of clamped edge which leads to more extension of the mid-plane. Therefore, it should be expected that deformations of the mid-plane play an important role in the natural frequencies. The all differences in these cases, as can be seen in Tables 3 and 4, are positive, *i.e.* the accurate natural frequencies are higher than those reported by Ref. [23]. This is because of the fact that the effect of in-plane displacement causes an increase in the stiffness of the plate. For the SSSF boundary condition and in all aspect ratios, the maximum (absolute value) of differences occurred in the power index $n = 1$ and the differences decrease with the increase of the power index. Interesting point about the SSSF is that, although discrepancies are not significant, approximately the all natural frequencies are lower than these reported by Ref. [23]. Natural frequencies of the SFSF and SCSF boundary

Table 4 Effect of in-plane displacements on non-dimensional fundamental frequency $\omega = \omega h \sqrt{\rho_c / E_c}$ of SCSC and SSSF Al / Al_2O_3 FG plate versus a/b and n ($h/a = 0.15$)

a/b	n	Hosseini-Hashemi <i>et al.</i> (2010)	SCSC	Difference (%)	Hosseini-Hashemi <i>et al.</i> (2010)	SSSF	Difference (%)
0.5	0	0.08729	0.08729	0	0.06713	0.06713	0
	0.25	0.07950	0.079905	0.51	0.06145	0.06138	-0.11
	1	0.06790	0.067110	-1.18	0.05346	0.051465	-3.876
	5	0.05695	0.057255	0.53	0.04568	0.044055	-3.688
1	0	0.16713	0.16714	0%	0.07537	0.07537	0
	0.25	0.14927	0.153705	2.88	0.06890	0.06894	0.058
	1	0.11955	0.129975	8.02	0.05968	0.05781	-3.235
	5	0.09479	0.109305	13.279	0.05078	0.04944	-2.71
2	0	0.41996	0.41996	0	0.10065	0.10066	0
	0.25	0.36112	0.389835	7.37	0.09170	0.092145	0.483
	1	0.26091	0.334605	22.02	0.07851	0.077325	-1.532
	5	0.19258	0.273345	29.55	0.06610	0.06588	-0.334

Table 5 Effect of in-plane displacements on non-dimensional fundamental frequency $\omega = \omega h \sqrt{\rho_c / E_c}$ of SFSF and SCSF Al / Al_2O_3 FG plate versus a/b and n ($h/a = 0.15$)

a/b	n	Hosseini-Hashemi <i>et al.</i> (2010)	SFSF	Difference (%)	Hosseini-Hashemi <i>et al.</i> (2010)	SCSF	Difference (%)
0.5	0	0.06364	0.06364	0	0.06781	0.06781	0
	0.25	0.05829	0.058185	-0.18	0.06205	0.06201	-0.064
	1	0.05080	0.04878	-4.14	0.05391	0.05199	-3.69
	5	0.04349	0.041775	-4.105	0.04600	0.044505	-3.36
1	0	0.06290	0.06291	0	0.08062	0.08062	0
	0.25	0.05761	0.05751	-0.174	0.07351	0.07378	0.366
	1	0.05021	0.04821	-4.148	0.06308	0.06195	-1.824
	5	0.04301	0.041295	-4.153	0.05322	0.05286	-0.681
2	0	0.06217	0.062175	0	0.13484	0.13485	0
	0.25	0.05695	0.056835	-0.202	0.12160	0.123735	1.725
	1	0.04970	0.04764	-4.32	0.10066	0.10422	3.415
	5	0.04262	0.040815	-4.42	0.08226	0.08814	6.67

condition for several aspect ratios and power law indices were presented in the Table 5 and compared with those reported by Ref. [23]. The maximum differences of SFSF boundary condition for aspect ratios of 0.5, 1 and 2 occurred in the power index 1, 5 and 5 respectively. The all frequencies are lower than those reported in Ref. [23]. The differences are not significant and it could be stated that in this boundary condition neglecting the in-plane displacement is an acceptable approximation. The maximum differences (absolute value) of aspect ratios 0.5, 1 and 2 for SCSF boundary condition occur in the power index 1, 1 and 5, respectively. What can be observed until now is that presence of the free edge condition leads to lowering the frequency and the reduction is not noteworthy. Reasons could be originated from the nature of free edge condition which helps the mid-plate to conveniently deform. In Tables 6 through 8, the natural

Table 6 Effect of in-plane displacements on non-dimensional fundamental frequency $\omega = \omega h \sqrt{\rho_c / E_c}$ of SSSS and SSSC Al/ZrO_2 FG plate versus h/a and n ($a/b = 1.5$)

h/a	n	Hosseini-Hashemi <i>et al.</i> (2010)	SSSS	Difference (%)	Hosseini-Hashemi <i>et al.</i> (2010)	SSSC	Difference (%)
0.05	0	0.02392	0.02392	0	0.03129	0.0312991	0
	0.25	0.02269	0.023077	1.67	0.02899	0.0302102	4.04
	1	0.02156	0.0220141	2.106	0.02667	0.0288259	7.48
	5	0.02180	0.0224614	2.944	0.02677	0.0293661	8.84
0.1	0	0.09188	0.09188	0	0.11639	0.116401	0
	0.25	0.08603	0.0887821	3.1	0.10561	0.1126532	6.252
	1	0.08155	0.0847642	3.792	0.09734	0.1076899	9.61
	5	0.08171	0.0860304	5.021	0.09646	0.1086353	11.21
0.2	0	0.32284	0.32285	0	0.37876	0.3787633	0
	0.25	0.31003	0.3132276	1.02	0.36117	0.3686341	2.02
	1	0.29399	0.2998908	1.967	0.33549	0.3538793	5.196
	5	0.29099	0.2998908	2.968	0.32783	0.3498276	6.288

Table 7 Effect of in-plane displacements on non-dimensional fundamental frequency $\omega = \omega h \sqrt{\rho_c / E_c}$ of SCSC and SSSF Al/ZrO_2 FG plate versus h/a and n ($a/b = 1.5$)

h/a	n	Hosseini-Hashemi <i>et al.</i> (2010)	SCSC	Difference (%)	Hosseini-Hashemi <i>et al.</i> (2010)	SSSF	Difference (%)
0.05	0	0.04076	0.0407615	0	0.01024	0.0102473	0.071
	0.25	0.03664	0.0393771	6.95	0.00981	0.0098844	0.753
	1	0.03250	0.0375876	13.53	0.00948	0.0094286	-0.545
	5	0.03239	0.038187	15.18	0.00963	0.0096311	0.011
0.1	0	0.14580	0.1458093	0	0.04001	0.040021	0.027
	0.25	0.12781	0.1413863	9.602	0.03810	0.0386428	1.405
	1	0.11453	0.1353763	15.398	0.03679	0.0368702	0.218
	5	0.11234	0.1356126	17.161	0.03718	0.0375454	0.973
0.2	0	0.43939	0.4394032	0	0.14871	0.14872	0
	0.25	0.41624	0.4289026	2.952	0.14354	0.1439017	0.251
	1	0.37962	0.4126960	8.015	0.13851	0.1375203	-0.719
	5	0.36695	0.4037823	9.122	0.13888	0.1388371	-0.031

Table 8 Effect of in-plane displacements on non-dimensional fundamental frequency $\omega = \omega h \sqrt{\rho_c / E_c}$ of SFSF and SCSF Al/ZrO_2 FG plate versus h/a and n ($a/b = 1.5$)

h/a	n	Hosseini-Hashemi <i>et al.</i> (2010)	SFSF	Difference (%)	Hosseini-Hashemi <i>et al.</i> (2010)	SCSF	Difference (%)
0.05	0	0.00719	0.00719	0	0.01249	0.0124926	0
	0.25	0.00692	0.0069385	0.267	0.01185	0.0120537	1.69
	1	0.00674	0.0066177	-1.85	0.01132	0.0114966	1.54
	5	0.00685	0.0067612	-1.314	0.01146	0.011733	2.33
0.1	0	0.02835	0.02836	0	0.04817	0.0481811	0
	0.25	0.02717	0.0273656	0.715	0.04532	0.0465435	2.63
	1	0.02641	0.0260995	-1.19	0.04327	0.0444333	2.62
	5	0.02677	0.0266228	-0.553	0.04352	0.0451254	3.56
0.2	0	0.10795	0.1079769	0	0.17323	0.17324	0
	0.25	0.10436	0.1043642	0	0.16671	0.1642275	-1.51
	1	0.10127	0.0996710	-1.604	0.15937	0.1606148	0.77
	5	0.10200	0.1009878	-1	0.15878	0.1612901	1.556

frequencies of Al/ZrO_2 FG plate for the aspect ratio of 1.5 and several thickness-length ratios, power indices and boundary conditions are presented. It can be deduced from these table that except the SSSC and SCSC boundary conditions, in all the other boundary conditions *i.e.* SSSF, SFSF, SCSF and SSSS, the effect of in-plane displacements on the natural frequencies are not significant. Remarkable point in these tables is that the maximum (absolute value) of differences in all boundary conditions, with the exception of the SFSF case, occur in $h/a = 0.1$. With the increase of h/a , the differences decrease. It could be due to fact that when the thickness of the plate increases, the effect of in-plane deformations on the overall stiffness of the plate is reduced. The maximum differences in the SCSF, SCSC, SSSC and SSSS boundary conditions occurs in the power index 1 and $h/a = 0.1$, in SSSF occurs in power index 0.25 and $h/a = 0.1$, and in SFSF occurs in the power index 1 and $h/a = 0.05$. The differences for the SCSC, SSSC and SSSS are positive and for the other boundary conditions are positive or negative. It can be concluded from Tables 3 through 8 that for the boundary conditions which at least have a clamped edge, the assumption of neglecting the in-plane displacement is not an acceptable approximation. As it can be seen from the tables, in some cases, the differences of about 30% were observed. This error is not acceptable for engineering applications.

The natural frequencies for various boundary conditions versus h/a and mode number with $n = 1$, $a/b = 1$ are presented in the Table 9. The important phenomena which is presented in this table is that the mode of vibration could be changed by variation of h/a . This matter can be seen for various boundary conditions. For example, in the SCSC, SSSC, SCSF and SSSF boundary conditions with the increase of h/a from 0.1 to 0.2, the third mode of vibration is changed from (2, 2) to (1, 3). In the SSSS boundary condition, the increase of h/a from 0.05 to 0.1 changes the third mode of vibration from (2, 2) to (1, 3).

The natural frequencies for various boundary conditions versus a/b and mode number with $n = 1$, $h/a = 0.1$ are presented in the Table 10. Similar to the Table 9, in this table the change of mode of vibration with variations of a/b are observed. In the SCSC boundary condition, with the increase of a/b from 0.5 to 1 and 1 to 2 the third mode of vibration is changed from (1,3) to (2,2) and from (2,2) to (3,1) and the second mode of vibration is changed form (1,2) to (2,1). The SSSC boundary condition has similar behavior. The situation is slightly different for the SCSF, SSSF and SFSF boundary conditions. In the SCSF boundary condition, with the increase of a/b from 0.5 to 1 and from 1 to 2 the third mode of vibration is changed from (1,3) to (2,2) and from (2,2) to (3,1), respectively. Moreover, in the SFSF boundary condition with the increase of a/b from 0.5 to 1 and from 1 to 2, the second mode of vibration is changed from (1,2) to (2,1) and then from (2,1) to (1,2) and the third mode of vibration is changed from (2,2) to (1,3). Also in the SSSF boundary condition with the increase of a/b from 0.5 to 1 and from 1 to 2, the third mode of vibration is

Table 9 The non-dimensional natural frequencies $\varpi = \omega h \sqrt{\frac{\rho_c}{E_c}}$ of Al/Al_2O_3 FG plate with various boundary conditions versus h/a and mode number (M. N.) ($n = 1, a/b = 1$)

h/a	M. N.	SSSS	SCSC	SCSF	SFSF	SSSC	SSSF
0.05	1	0.011310 (1,1)	0.016400 (1,1)	0.007255 (1,1)	0.005535 (1,1)	0.013485 (1,1)	0.006700 (1,1)
	2	0.027940 (1,2)	0.030765 (2,1)	0.018650 (1,2)	0.009170 (1,2)	0.029170 (2,1)	0.015750 (1,2)
	3	0.044195 (2,2)	0.052040 (2,2)	0.035195 (2,2)	0.020670 (1,3)	0.047840 (2,2)	0.033165 (2,2)
0.1	1	0.044200 (1,1)	0.062230 (1,1)	0.028400 (1,1)	0.021850 (1,1)	0.052040 (1,1)	0.026340 (1,1)
	2	0.105900 (1,2)	0.114720 (2,1)	0.070790 (1,2)	0.035680 (1,2)	0.109820 (2,1)	0.060700 (1,2)
	3	0.162020 (1,3)	0.185430 (2,2)	0.130320 (2,2)	0.078620 (1,3)	0.173720 (2,2)	0.124120 (2,2)
0.2	1	0.163100 (1,1)	0.212160 (1,1)	0.106040 (1,1)	0.083540 (1,1)	0.185440 (1,1)	0.099620 (1,1)
	2	0.323600 (1,2)	0.378260 (2,1)	0.242480 (1,2)	0.131420 (1,2)	0.368660 (2,1)	0.216520 (1,2)
	3	0.360380 (1,3)	0.545980 (1,3)	0.344680 (1,3)	0.245400 (1,3)	0.394960 (1,3)	0.283140 (1,3)

Table 10 The non-dimensional natural frequencies $\varpi = \omega h \sqrt{\frac{\rho_c}{E_c}}$ of Al/Al_2O_3 FG plate with various boundary conditions versus a/b and mode number (M. N.) ($n = 1, h/a = 0.1$)

a/b	M. N.	SSSS	SCSC	SCSF	SFSF	SSSC	SSSF
0.5	1	0.027940 (1,1)	0.030770 (1,1)	0.023610 (1,1)	0.022110 (1,1)	0.029170 (1,1)	0.023350 (1,1)
	2	0.044200 (1,2)	0.052040 (1,2)	0.035200 (1,2)	0.026340 (1,2)	0.047840 (1,2)	0.033170 (1,2)
	3	0.070520 (1,3)	0.082970 (1,3)	0.056550 (1,3)	0.089050 (2,2)	0.076510 (1,3)	0.052260 (1,3)
1	1	0.044200 (1,1)	0.062230 (1,1)	0.028400 (1,1)	0.021850 (1,1)	0.052040 (1,1)	0.026340 (1,1)
	2	0.105900 (1,2)	0.114720 (2,1)	0.070790 (1,2)	0.084540 (2,1)	0.109820 (2,1)	0.060700 (1,2)
	3	0.162020 (1,3)	0.185430 (2,2)	0.130320 (2,2)	0.078620 (1,3)	0.173720 (2,2)	0.124120 (2,2)
2	1	0.105900 (1,1)	0.177380 (1,1)	0.049200 (1,1)	0.021590 (1,1)	0.139210 (1,1)	0.035680 (1,1)
	2	0.162020 (1,2)	0.212160 (2,1)	0.106030 (1,2)	0.057870 (1,2)	0.185430 (2,1)	0.099610 (2,1)
	3	0.273730 (1,3)	0.280470 (3,1)	0.196210 (3,1)	0.089830 (1,3)	0.264200 (3,1)	0.154280 (1,3)

changed from (1,3) to (2,2) and from (2,2) to (1,3) and the second mode of vibration is changed from (1,2) to (2,1).

Figure 2 shows the variation of natural frequencies for a SCSC plate versus the thickness-length ratio for several power law indices. As it also expected, the natural frequency increases with increasing the thickness-length ratio. In smaller value of thickness-length ratio, the effect of power law index on natural frequency is negligible. However, as the thickness-length ratio increases, this effect increases. It also should be mentioned that a reduction in natural frequencies is observed with increasing the power law index.

6. CONCLUSIONS

Free vibration of FG rectangular plates has been studied by means of the first order shear deformation plate theory. The governing equations of motion have been obtained without any simplifications or extra assumptions on mid-plane displacements. The equations have been solved using Levy's method for the

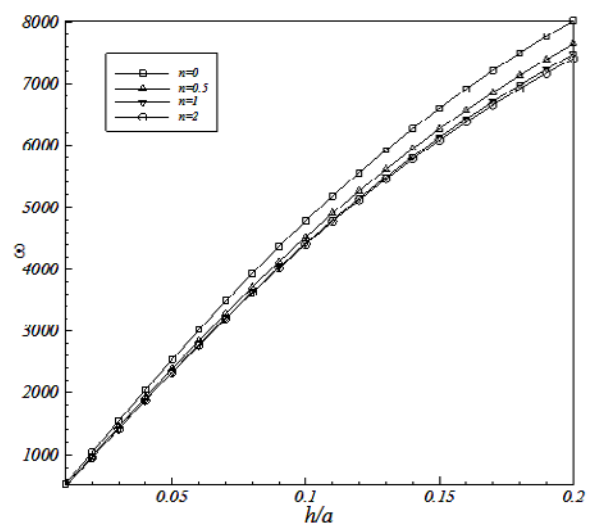


Fig. 2 The fundamental natural frequency of FG rectangular plate versus the thickness-length ratio for SCSC boundary condition ($a/b = 1$)

combination of clamped, simply supported and free edge boundary conditions. The results have been compared with the case which the in-plane displacements were neglected. As can be concluded from the results, in the SFSF, SCSF and SSSF boundary conditions, the differences are not significant and it can be concluded that neglecting the in-plane displacement in the mentioned boundary conditions practically is a good approximation. Also it is worthy to mention that the presence of the free edge condition leads to lowering the frequency and the reduction is not noteworthy. In the SSSS boundary condition, only for aspect ratio of 2 and power law index 5 the difference becomes important. As the results show, ignoring the in-plane displacements in case of SSSC and SCSC boundary conditions is not a good engineering approximation. It has been observed that the differences for larger aspect ratios and/or larger power law indices are more severe. Variations of natural frequencies with the thickness-length ratio show remarkable patterns. With variation of thickness-length ratio from 0.05 to 0.2 the differences in some boundary conditions have a maximum which the major of them occurs in the thickness-length ratio 0.1. It could be due to fact that when the thickness of the plate increases, the effect of in-plane deformations on the overall stiffness of the plate is reduced. Also, it should be mentioned that the results show change of the modes of vibration with the variation of aspect ratio and/or thickness-length ratio.

NOMENCLATURES

- a = length of rectangular plate
 A_{ij}, B_{ij}, D_{ij} = material stiffness coefficients of the plate ($i = 1, 3; j = 1, 2, 3$)
 b = width of rectangular plate
 $E(z)$ = elasticity modulus of functionally graded material (FGM)
 E_m, E_c = elasticity modulus of metal and ceramic, respectively
 h = plate thickness
 I_0, I_1, I_2 = inertia terms
 k^2 = shear correction factor
 M_{xx}, M_{yy}, M_{xy} = bending and twisting moment intensities
 N_{xx}, N_{yy}, N_{xy} = in-plane resultant forces
 n = power law index
 Q_x, Q_y = out of plane resultant forces
 u, v, w = displacements components in x, y and z directions, respectively
 $\varepsilon_{xx}, \varepsilon_{yy}$ = normal strains components
 $\varepsilon_{xy}, \varepsilon_{xz}, \varepsilon_{yz}$ = shear strains components
 ν = Poisson ratio
 σ_{xx}, σ_{yy} = normal stress components
 $\sigma_{xy}, \sigma_{xz}, \sigma_{yz}$ = shear stress components
 $\rho(z)$ = density of FG plate
 ω_m = m^{th} frequency of vibration
 Ψ_x, Ψ_y = rotation functions of middle surface

REFERENCES

1. Yamanouchi, M., Koizumi, M., Hirai, T. and Shiota, I., *Proceedings of First International Symposium on Functionally Graded Materials*, Japan, Sendai, (1990).
2. Reddy, J. N., "Analysis of Functionally Graded Plates," *International Journal for Numerical Methods in Engineering*, **47**, pp. 663–684 (2000).
3. Birman, V. and Byrd, L. W., "Modeling and Analysis of Functionally Graded Materials and Structures," *Journal of Applied Mechanics*, ASME, **60**, pp. 195–216 (2007).
4. Fukui, Y., "Fundamental Investigation of Functionally Graded Material Manufacturing System Using Centrifugal Force," *International Journal of the Japan Society for Mechanics Engineering*, **4**, pp. 144–148 (1991).
5. Yang, J. and Shen, H. S., "Dynamic Response of Initially Stressed Functionally Graded Rectangular Thin Plates," *Composite Structures*, **54**, pp. 497–508 (2001).
6. He, X. Q., Ng, T. Y., Sivashanker, S. and Liew, K. M., "Active Control of FGM Plates with Integrated Piezoelectric Sensors and Actuators," *International Journal of Solids and Structures*, **38**, pp. 1641–1655 (2001).
7. Qian, L. F., Batra, R. C. and Chen, L. M., "Static and Dynamic Deformations of Thick Functionally Graded Elastic Plates by Using Higher-Order Shear and Normal Deformable Plate Theory and Meshless Local Petrov–Galerkin Method," *Composites: Part B*, **35**, pp. 685–697 (2004).
8. Vel, S. S. and Batra, R. C., "Three-Dimensional Exact Solution for the Vibration of Functionally Graded Rectangular Plates," *Journal of Sound and Vibration*, **272**, pp. 703–730 (2004).
9. Kim, Y. W., "Temperature Dependent Vibration Analysis of Functionally Graded Rectangular Plates," *Journal of Sound and Vibration*, **284**, pp. 531–549 (2005).
10. Shiau, L. C. and Zeng, J. Y., "Free Vibration of Rectangular Plate with Delamination," *Journal of Mechanics*, **26**, pp. 87–93 (2010).
11. Ferreira, A. J. M., Batra, R. C., Roque, C. M. C., Qian, L. F. and Jorge, R. M. N., "Natural Frequencies of Functionally Graded Plates by a Mesh Less Method," *Composite Structures*, **75**, pp. 593–600 (2006).
12. Sundararajan, N., Prakash, T. and Ganapathi, M., "Nonlinear Free Flexural Vibrations of Functionally Graded Rectangular and Skew Plates Under Thermal Environments," *Finite Elements in Analysis and Design*, **42**, pp. 152–168 (2005).
13. Woo, J., Meguid, S. A. and Ong, L. S., "Nonlinear Free Vibration Behavior of Functionally Graded Plates," *Journal of Sound and Vibration*, **289**, pp.

- 595–611 (2006).
14. Gilhooley, D. F., Batra, R. C., Xiao, J. R., McCarthy, M. A. and Gillespie, J. W., “Analysis of Thick Functionally Graded Plates by Using Higher-Order Shear and Normal Deformable Plate Theory and MLPG Method with Radial Basis Functions,” *Composite Structures*, **80**, pp. 539–552 (2007).
 15. Matsunaga, H., “Free Vibration and Stability of Functionally Graded Plates According to a 2-D Higher-Order Deformation Theory,” *Composite Structures*, **82**, pp. 499–512 (2008).
 16. Zhang, D. G. and Zhou, Y. H., “A Theoretical Analysis of FGM Thin Plates Based on Physical Neutral Surface,” *Computational Materials Science*, **44**, pp. 716–720 (2008).
 17. Fares, M. E., Elmarghany, M. K. and Atta, D., “An Efficient and Simple Refined Theory for Bending and Vibration of Functionally Graded Plates,” *Composite Structures*, **91**, pp. 296–305 (2009).
 18. Malekzadeh, P., “Three-Dimensional Free Vibration Analysis of Thick Functionally Graded Plates on Elastic Foundations,” *Composite Structures*, **89**, pp. 367–373 (2009).
 19. Wu, C. P. and Lu, Y. C., “A Modified Pagano Method for the 3D Dynamic Responses of Functionally Graded Magneto-Electro-Elastic Plates,” *Composite Structures*, **90**, pp. 363–372 (2009).
 20. Li, Q., Iu, V. P. and Kou, K. P., “Three-Dimensional Vibration Analysis of Functionally Graded Material Plates in Thermal Environment,” *Journal of Sound and Vibration*, **324**, pp. 733–750 (2009).
 21. Liu, D. Y., Wang, C. Y. and Chen, W. Q., “Free Vibration of FGM Plates with In-Plane Material Inhomogeneity,” *Composite Structures*, **92**, pp. 1047–1051 (2010).
 22. Zhao, X., Lee, Y. Y. and Liew, K. M., “Free Vibration Analysis of Functionally Graded Plates Using the Element-Free Kp-Ritz Method,” *Journal of Sound and Vibration*, **319**, pp. 918–939 (2009).
 23. Hosseini-Hashemi, Sh., Rokni Damavandi Taher, H., Akhavan, H. and Omidi, M., “Free Vibration of Functionally Graded Rectangular Plates Using First-Order Shear Deformation Plate Theory,” *Applied Mathematical Modelling*, **34**, pp. 276–290 (2010).
 24. Hosseini-Hashemi, Sh., Fadaee, M. and Atashipour, S. R., “A New Exact Analytical Approach for Free Vibration of Reissner–Mindlin Functionally Graded Rectangular Plates,” *International Journal of Mechanical Sciences*, **53**, pp. 11–22 (2011).
 25. Hosseini-Hashemi, Sh., Fadaee M. and Atashipour S. R., “A Study on the Free Vibration of Thick Functionally Graded Rectangular Plates According to a New Exact Closed-Form Procedure,” *Composite Structures*, **93**, pp. 722–735 (2011).
 26. Reddy, J. N., *Energy Principles and Variational Methods in Applied Mechanics*, 2nd Edition, John Wiley and Sons Inc, New York (2002).
 27. Reddy, J. N., *Theory and Analysis of Elastic Plates*, Taylor & Francis, Philadelphia (1999).

(Manuscript received September 14, 2011, accepted for publication November 1, 2012.)